The nuclear receptor *NR2E3* plays a role in human retinal photoreceptor differentiation and degeneration

Ann H. Milam*†‡, Linda Rose*, Artur V. Cideciyan*, Mark R. Barakat*, Wai-Xing Tang*, Nisha Gupta*, Tomas S. Aleman*, Alan F. Wright§, Edwin M. Stone¶, Val C. Sheffield‖, and Samuel G. Jacobson*

*Scheie Eye Institute and †F. M. Kirby Center for Molecular Ophthalmology, University of Pennsylvania, Philadelphia, PA 19104; §Medical Research Council Human Genetics Unit, Western General Hospital, Edinburgh, EH4 2XU Scotland; and ¶Department of Ophthalmology and Visual Science, and ‖Department of Pediatrics and the Howard Hughes Medical Institute, University of Iowa, Iowa City, IA 52242

Edited by Jeremy Nathans, The Johns Hopkins University School of Medicine, Baltimore, MD, and approved November 19, 2001 (received for review October 4, 2001)

Normal human retinal development involves orderly generation of rods and cones by complex mechanisms. Cell-fate specification involves progenitor cell lineage and external signals such as soluble factors and cell–cell interactions. In most inherited human retinal degenerations, including retinitis pigmentosa, a mutant gene causes loss of visual function, death of mature rods, and eventually death of all cone subtypes. Only one inherited retinal disorder, the enhanced S cone syndrome (ESCS), shows increased visual function, involving the minority S (blue) cones, and decreased rod and L/M (red/green) cone function. This autosomal recessive disease is caused by mutations in *NR2E3*, a photoreceptor nuclear receptor transcription factor, and may result from abnormal cell-fate determination, leading to excess S cones at the expense of other photoreceptor subtypes. In 16 ESCS patients with the most common *NR2E3* mutation, R311Q, we documented an abnormal ratio of S to L/M cone function and progressive retinal degeneration. We studied the postmortem retina of an ESCS patient homozygous for *NR2E3* R311Q. No rods were identified, but cones were increased approximately 2-fold, and 92% were S cones. Only 15% of the cones expressed L/M cone opsin, and some coexpressed S cone opsin. The retina was disorganized, with densely packed cones intermixed with inner retinal neurons. The retina was also degenerate, retaining photoreceptors in only the central and far peripheral regions. These observations suggest a key role for *NR2E3* in regulation of human photoreceptor development. Degeneration of the *NR2E3* retina may result from defective development, known S cone fragility, or abnormal maintenance of mature photoreceptors.

The molecular events during development of invertebrate and vertebrate retinas are incompletely understood. The specification of rods and cones involves interactions of both intrinsic and extrinsic factors, including cell lineage, soluble factors, and local cell–cell interactions (1–3). These complex signaling pathways involve nuclear receptors, a superfamily of transcription factors that share structural features, including DNA and ligand-binding domains (4, 5). A human photoreceptor-specific nuclear receptor (*PNR*), *NR2E3*, is a member of the nuclear receptor subfamily II (6). Coexpression of *NR2E3*, *CRX* (cone-rod homeobox; ref. 7), and *NRL* (nuclear retina leucine zipper; ref. 8) in human Y79 retinoblastoma cells suggests that *NR2E3* is a component of a photoreceptor transcription cascade in human retinal development (6).

Mutations in *NR2E3* (9, 10) cause a unique human retinal disease, the enhanced S cone syndrome (ESCS), initially described using psychophysical and electrophysiological methods (11). ESCS patients lack rod photoreceptor function, like other inherited retinal degenerations such as retinitis pigmentosa (12), but are unique because their S (blue) cones, normally a minority population (13), are more responsive to light than the usually more populous L/M (red/green) cones (11, 14–16). The retinal pathology underlying the ESCS phenotype is not known. Noninvasive measurement of photoreceptor physiology (16) and the recent molecular association (9) have led to speculation that an *NR2E3* mutant retina could resemble transplants and explants of rabbit and rodent retinas, which develop a high S to M cone ratio (17). Mutant *NR2E3* may result in disordered retinal cell-fate determination, with overproduction of S cones at the expense of other photoreceptor types (9, 18).

An essential next step to understand the consequence of mutant *NR2E3* in patients is to perform histopathology on a human retina with ESCS (18). In the present study, we used immunocytochemical and morphometric techniques to investigate a postmortem retina from a patient diagnosed previously with ESCS caused by the most common (R311Q) *NR2E3* mutation. We found a dramatic increase in the S cone population, a 2-fold increase in total numbers of cones, some of which coexpress S and L/M opsin, and a disorganized, degenerate inner retina. These findings in humans extend the observations in retinas of mutant *Nr2e3 rd7/rd7* mice, which show overproduction of S cones and retinal degeneration (19, 20). *NR2E3* may play a key role in the developmental processes that lead to normal human photoreceptor topography. The abnormal photoreceptor pattern we document here may be a useful phenotypic marker in future studies of the molecular pathways that regulate normal retinal development.

Materials and Methods

Subjects. Normal subjects and patients with ESCS caused by *NR2E3* mutations were included in the study. Molecular studies on these patients have been published (9, 10). Informed consent was obtained from subjects after explanation of the procedures; all studies conformed to institutional guidelines and the Declaration of Helsinki.

Phenotype. The patients were studied with clinical ocular examination and visual function tests, including kinetic perimetry, electroretinography (ERG), and spectral static threshold perimetry. S cone function was measured with 440 nm stimuli on a yellow background (170 cd·m^{-2}). In patients, L/M cone function was determined with 650 nm of stimuli in the dark-adapted state because of the major losses of rod sensitivity in ESCS (11). In normals, L/M cone function was determined during the cone plateau phase after a bleach. In analyses of cross-sectional data,

This paper was submitted directly (Track II) to the PNAS office.

Abbreviations: ESCS, enhanced S cone syndrome; ERG, electroretinography; RPE, retinal pigment epithelium; INL, inner nuclear layer.

‡To whom reprint requests should be addressed. E-mail: annmilam@mail.med.upenn.edu.

The publication costs of this article were defrayed in part by page charge payment. This article must therefore be hereby marked "*advertisement*" in accordance with 18 U.S.C. §1734 solely to indicate this fact.

only retinal loci with measurable S and L/M cone function were considered. In serial data, only retinal loci were considered that had measurable S and L/M cone function at all time points. ERGs were evoked with white flashes (5.4 cd·s·m^{-2}), and a-wave amplitude was measured conventionally from baseline to trough. Details of these visual function techniques and analysis methods have been published (11, 14, 16, 21, 22).

Histopathology. Postmortem human eyes were obtained through the Foundation Fighting Blindness (FFB, Owings Mills, MD). The right eye from a 77-year-old woman with ESCS (FFB 595) was fixed 5 h postmortem in a mixture of 4% paraformaldehyde and 0.5% glutaraldehyde in 0.1 M phosphate buffer, pH 7.3. As controls, a normal eye (FFB 616, 49 years old, fixed at 8.5 h postmortem) and an eye with retinitis pigmentosa caused by the threonine-17-methionine rhodopsin mutation (23) were processed in the same way. Retinal samples from the macula, midperiphery, and far periphery were embedded in glycol methacrylate, sectioned at 4 μm, and stained with Richardson's methylene blue/azure II.

Immunocytochemistry. Samples including the peripapillary retina and optic nerve head, midperiphery, and far periphery were cryosectioned at 12 μm and processed for immunofluorescence (24–26).

Antibodies and specificity were mouse mAb 7G6, cone cytoplasm (1:250; P. MacLeish, Morehouse School of Medicine, Atlanta); mouse mAb anti-rhodopsin, rod outer segments (4D2 and 1D4, 1:40; R. Molday, Univ. of British Columbia, Vancouver, BC, Canada); sheep pAb anti-rhodopsin (1:1,000; D. Papermaster, Univ. of Connecticut Health Center, Farmington); mouse mAb anti-rds/peripherin, rod/cone outer segments (3B6, undiluted; R. Molday); rabbit pAb anti-L/M cone opsin (UW-16, 1:500; J. Saari, Univ. of Washington, Seattle); rabbit pAb anti-S cone opsin (JH455, 1:5,000; J. Nathans, The Johns Hopkins Medical School, Baltimore); mouse mAb anti-S cone opsin (OS-2, 1:1,000; A. Szel, Semmelweis Univ. Medical School, Budapest); rhodamine-conjugated peanut agglutinin lectin, cone outer segments and sheaths (PNA, 1:100; Vector Laboratories); rabbit pAb anti-recoverin, rods, cones, and cone bipolar cells (P26, 1:1,000; A. Dizhoor, Wayne State Univ., Detroit); mouse mAb anti-calbindin, L/M cones, horizontal, bipolar, and amacrine cells (C8666, 1:200; Sigma); rabbit pAb anti-cholecystokinin precursor, S cone ON-bipolar cells (R6B6, 1:1,000; J. Del Valle, Univ. of Michigan, Ann Arbor); rabbit pAb anti-γ-aminobutyric acid, amacrine cells (1:100; R. Marc, Univ. of Utah, Salt Lake City); mouse mAb anti-SV2, synaptic vesicles (1:400; K. Buckley, Harvard Medical School, Boston); rabbit pAb anticellular retinaldehyde-binding protein, retinal pigment epithelium (RPE), and Müller cells (1:100; J. Saari); and rabbit pAb anti-glial fibrillary acidic protein, astrocytes, and reactive Müller cells (1:750, Dako).

Secondary antibodies (goat anti-rabbit, anti-mouse, or anti-sheep IgG, 1:50) were labeled with Alexa Fluor 488 (green; Molecular Probes), Cy-2 (green), or Cy-3 (red) (Jackson ImmunoResearch). Cell nuclei were stained with 4′,6′-diamidino-2-phenylindole (blue, 1 μg/ml; Molecular Probes). Control sections were treated in the same way with omission of primary antibody.

Immunolabeled sections were examined with a Leica DMR microscope equipped for epifluorescence or a Leica TCS SP11 laser-scanning confocal microscope. Images were imported into Adobe PHOTOSHOP 5.0, and dye-sublimation prints were generated.

Morphometry. Overlapping photomicrographs were made with a $\times$20 objective of every fifth section of the ESCS retina just inferior to the optic nerve head, a region that contained numerous S cones with outer segments. This was the only region available for immunocytochemistry, as most of the central retina had been processed for routine histopathology (see Fig. 2*A*) before we learned that the donor had ESCS and an *NR2E3* mutation. Thirteen sections of this region, each 600 μm wide, were quantified. Only well oriented sections were used that did not have oblique orientation of the photoreceptors. The same retinal region was counted in the normal and retinitis pigmentosa (23) retinas. The sections were immunolabeled with anti-S cone opsin, anti-L/M cone opsin, or mAb 7G6 (to label all cones). The images were scanned, and montages were prepared in Adobe PHOTOSHOP 5.0. Counts were made of cell bodies labeled with anti-S and/or anti-L/M cone opsin and with mAb 7G6. The data were expressed as the mean of each cell type per 600 μm of retinal length. The data were graphed, and SEMs were calculated with Microsoft EXCEL 98.

Results

Phenotype of the *NR2E3* R311Q Genotype. Sixteen patients (ages 21–73 years, 11 probands and five affected siblings) were identified by visual function studies as having ESCS and later found to have an *NR2E3* mutation in codon 311. Of the 11 probands, six were homozygous for the *NR2E3* R311Q mutation, including the eye donor. Five probands were heterozygotes for the R311Q variation; two were compound heterozygotes (R311Q/R309G; R311Q/splice acceptor intron 1), and in three others, a second mutation has not been identified despite sequencing of the entire protein-coding region and all consensus splice sites of the gene. All patients showed ophthalmoscopic evidence of pigmentary retinopathy. Of the 16 patients, seven had either central or peripheral retinoschisis and two others had a history of retinal detachment requiring surgical repair in one eye. Visual acuity was subnormal (varying from 20/25 to worse than 20/400) in all but one patient. Kinetic visual fields were abnormal in 15 patients; 11 of 15 had measurable peripheral function, and four were reduced to a central island of function only. These four patients had no detectable ERG signals, whereas the others showed waveforms with greater S than L/M cone signals, as noted in other ESCS patients (11, 14–16, 21, 22).

Fig. 1*A* shows psychophysically measured sensitivities mediated by S and L/M cones and a ratio of S to L/M cone function in 14 of these patients; data have been divided in three annular retinal regions (*Inset*). In regions I and II, patients show a range of S cone sensitivities from supernormal to subnormal. Most patients retaining vision in the more peripheral region III showed supernormal S cone sensitivities. The decline in normal S cone sensitivity in the periphery emphasizes this effect. The patients showed abnormal L/M cone sensitivities across all regions of the retina. The ratio of S to L/M cone sensitivity is approximately 1 log unit greater than normal in the more central regions and nearly 2 log units greater than normal in the periphery.

Serial data over a decade for S and L/M cone function in an ESCS patient homozygous for the *NR2E3* R311Q mutation demonstrate the progressive nature of this retinopathy (Fig. 1*B*). The rate of sensitivity loss is similar for the two receptor systems, but there was greater loss of function in the more peripheral than central region. Direct evidence for progressive photoreceptor dysfunction in this patient was obtained with the ERG a-wave. The a-wave amplitude shows a decline over this time period (slope of -0.6 log per decade) (Fig. 1*C*). Kinetic perimetry results declined similarly over this interval (not shown). An 8-year interval between ERGs in another patient (heterozygous for the *NR2E3* R311Q mutation) also showed a-wave amplitude loss. Taken together, the spectral psychophysical and ERG measurements indicate that this *NR2E3* mutation causes not only

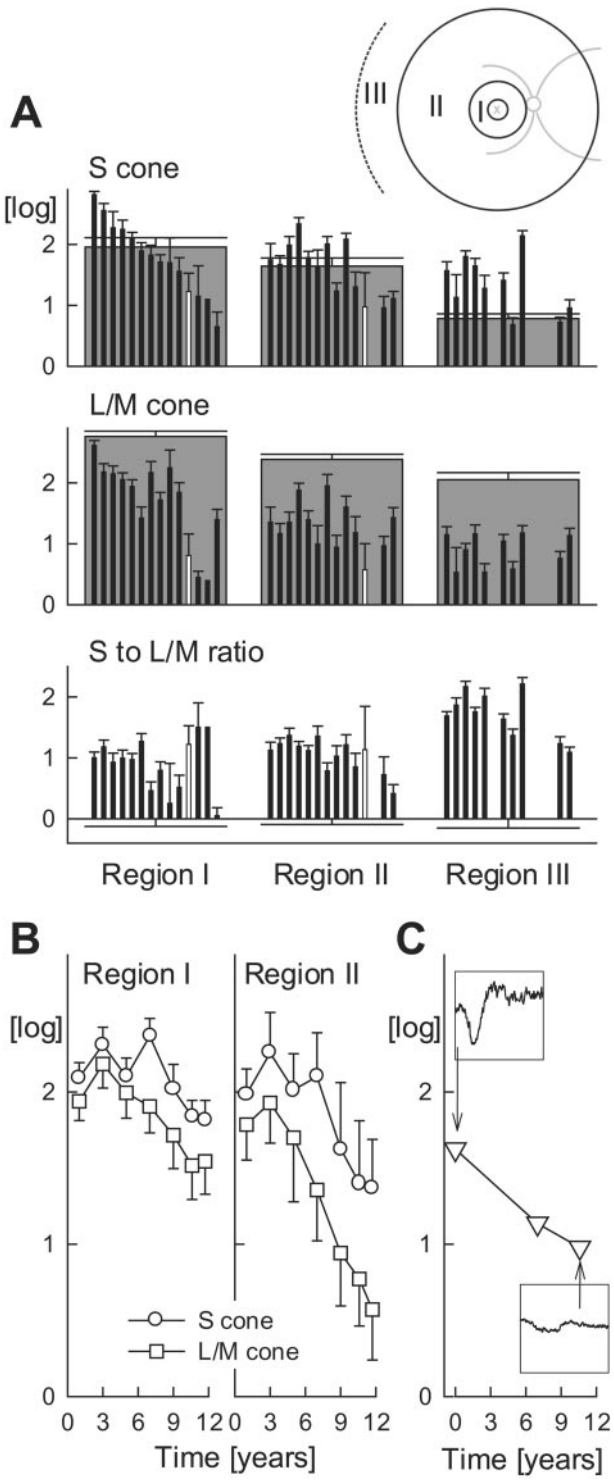

Fig. 1. S versus L/M cone function and disease progression in patients with *NR2E3* R311Q mutations. (*A*) Psychophysically measured S and L/M cone sensitivities and their ratio summarized over three annular regions corresponding to eccentricities of 3–10°, 10–34°, and >34°, respectively (I, II, III shown in *Inset*). Patient data (thin black bars) are ordered (left to right) in declining S cone sensitivity in region I. S to L/M cone sensitivity ratios are normalized by the mean normal ratio in each region. Data from the eye donor at age 70 years are shown as white. Normal data are gray except in the bottom row, where mean normal is 0 log. Error bars, 2 SEM. (*B*) Serial data over 11 years in a patient between the ages of 40 and 51 showing S and L/M cone sensitivities in regions I and II. (*C*) Serial dark-adapted ERG a-wave amplitudes in the same patient. *Insets* (ordinate range 100 μV; abscissa −10 to 160 ms) show two representative waveforms.

an abnormal ratio of S to L/M cone function but also progressive retinal degeneration.

***NR2E3* Proband-Eye Donor.** *In vivo* examination was performed when the proband-eye donor was age 70. She had previously been told her diagnosis was retinitis pigmentosa. There was parental consanguinity, and her 73-year-old sister also carried this diagnosis. The eye donor was homozygous for the *NR2E3* R311Q mutation. Her visual acuities at age 70 were <20/400, visual fields were reduced to a central island only, and ERGs were not detectable. Retinopathy was present throughout the fundus with prominent central and superior retinal clumps of black pigment. Retinoschisis was noted in the far inferior retinal periphery. Spectral psychophysical thresholds (Fig. 1*A*, white bar) indicated an abnormal ratio of S to L/M cone function, and the diagnosis was changed to ESCS. The 73-year-old sister of the proband was also studied, and she had similar ocular results to those of her sibling; spectral psychophysical thresholds indicated an abnormal S to L/M cone ratio (Fig. 1*A*, black bar next right from proband).

Gross pathology of the postmortem eye donor eye at age 77 showed a normal anterior segment. The optic nerve head was pale and waxy, and the retina was very thin, with a 360° ring of bone spicule pigment in the midperiphery. There were also clumps of black pigment in the central and superior retina.

Histopathology. The central part of the ESCS macula did not contain a recognizable fovea. The RPE was variably depigmented, and photoreceptors were reduced to 2–3 layers of nuclei (Fig. 2*A*) (normal is 6–8 layers) with short to absent outer segments. The outer plexiform layer was thin, and the inner nuclear layer (INL) varied in thickness. In places, the inner plexiform layer was interrupted by clusters of cells and radial fibers (Fig. 2*A*), and ganglion cells were reduced to an incomplete layer (normal is 6–8 layers). The nerve fiber layer was gliotic, and an epiretinal membrane was present. The midperiphery lacked photoreceptors and contained prominent bone spicule pigment (27). The far periphery retained a few photoreceptors, but the inner retina was degenerate.

Immunocytochemistry. No rods were identified in the ESCS retina by labeling with mAb or pAb anti-rhodopsin. Compared with the single row of cones in the normal central retina (Fig. 2*B*), the central part of the ESCS retina contained multiple layers of cones, identified with mAb 7G6 (Fig. 2*C*). The ESCS cones were densely packed with short outer segments, identified by labeling with anti-cone opsins (Fig. 2 *C–E*) and anti-rds/peripherin.

Virtually all cones were labeled with anti-S cone opsin (Fig. 2 *C–E*). A few cones were positive with anti-L/M cone opsin (Fig. 2*D*), some of which coexpressed S cone opsin (Fig. 2*D*). Both S and L/M cones had delocalized opsin in the surface membranes of their inner segments, cell bodies, axons, and synapses (Fig. 2 *C* and *D*). At the periphery of the macula, the cones were less densely packed and lacked outer segments (Fig. 2*E*). The RPE had been lost from these areas, and the cones showed variable loss of cytoplasmic immunoreactivity with mAb 7G6, anti-recoverin, and −SV2 (see ref. 28), consistent with ongoing cone cell degeneration.

The layering of the central retina was abnormal, with intermixing of cones with cells of the INL (Fig. 2 *A* and *E*). Some ectopic cones formed small rosettes around PNA-positive lumina. Where S cones were present in the INL, the inner plexiform layer, labeled by anti-SV2, was interrupted by radially coursing S cone and Müller cell processes (Fig. 2*E*). Because of its irregular thickness, we did not attempt to quantify individual cell types in the INL, but we noted some calbindin-positive horizontal and amacrine cells, anti-

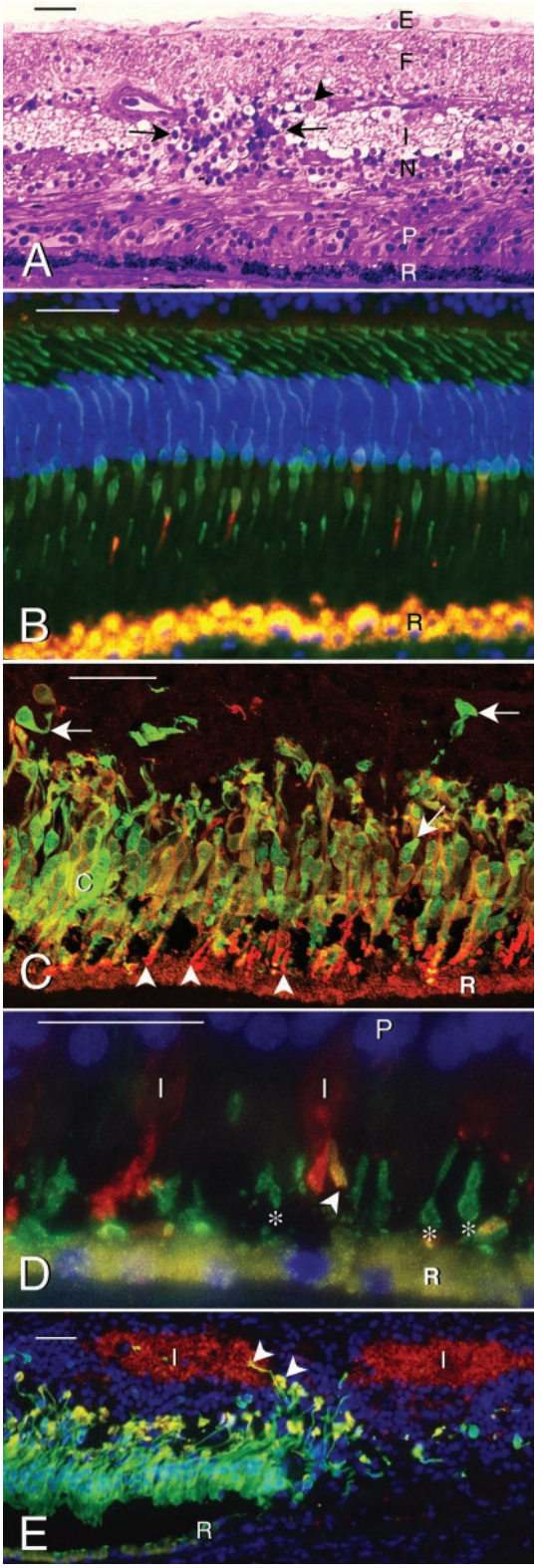

Fig. 2. Microscopy of normal and *NR2E3* mutant human retinas. The retinal pigment epithelium is indicated by (R). Bar indicates 50 μm in *A–C* and *E* and 25 μm in *D*. (*A*) Central macula of retina with *NR2E3* R311Q mutation. Glycol methacrylate section stained with Richardson's methylene blue/azure II. Photoreceptors (P) are reduced to 2–3 layers of nuclei (normal is 6–8 layers). Outer segments are short to absent. The inner nuclear layer (N) varies in thickness, and the inner plexiform layer (I) is interrupted by a cluster of cells and radial fibers (between arrows). Ganglion cells (arrowhead) are reduced to a discontinuous layer (normal is 6–8 layers), the nerve fiber layer (F) is gliotic, and an epiretinal membrane (E) is present. (*B–E*) Immunofluorescence images. The RPE (R) contains gold autofluorescent lipofuscin granules. The nuclei have been stained (blue) with 4′,6′-diamidino-2-phenylindole in *B*, *D*, and *E*. (*B*) Central part of normal human retina processed for immunofluorescence with mAb 7G6 (green), which labels the cytoplasm of all cones, and anti-S cone opsin (red), which labels four S cone outer segments. (*C*) Central part of ESCS retina labeled with mAb 7G6 (green), specific for cone cytoplasm, and anti-S cone opsin (red). Note multilayered cones (c) with outer segments (arrowheads) positive for S cone opsin. Most cones are double-labeled (gold) and have S cone opsin reactivity (red) in the surface membranes of the inner segments and cell bodies. A few 7G6 positive cones (arrows) are S cone opsin negative. (*D*) The *NR2E3* mutant retina labeled with anti-S cone opsin (green) (mAb OS-2, which labels S cone outer segments, indicated by *) and anti-L/M cone opsin (red). Note opsin delocalization to the inner segments (I) of the L/M cones and one cone outer segment (gold, arrowhead) that is positive for both L/M and S cone opsin. P, photoreceptor nuclei. (*E*) Low magnification micrograph showing loss of autofluorescent RPE (gold) and S-cones (green) from the periphery (right side) of the macula. The inner plexiform layer (I), labeled (red) with anti-SV2, is interrupted by S cones and their axons (arrowheads). R, edge of RPE.

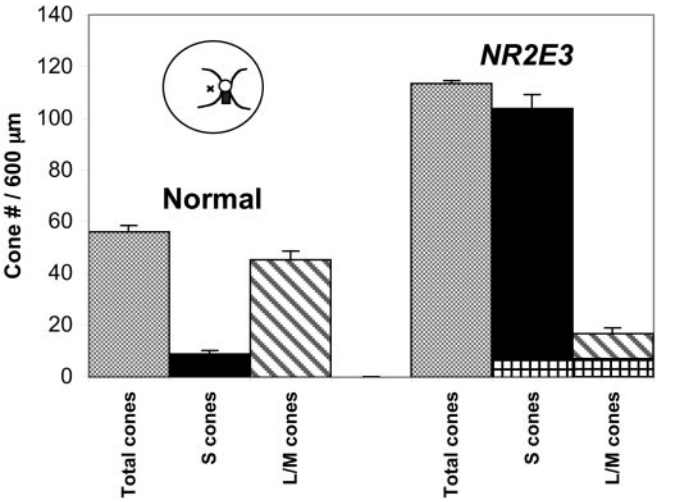

Fig. 3. Cone cell types in a normal and *NR2E3* mutant retina, identified by immunocytochemistry with mAb 7G6 (to label all cones), anti-S cone opsin (to label blue cones), and anti-L/M cone opsin (to label red/green cones). The cone counts are expressed per 600-μm length of retina. Compared with the normal retina, the *NR2E3* mutant shows an approximately 2-fold increase in total cones, the majority of which are S cones. The L/M cones are decreased in the *NR2E3* mutant retina, and some cones (crosshatched bars) coexpress L/M and S cone opsin. The retinal sections were taken from a region (black rectangle in cartoon of fundus) just inferior to the optic nerve head (small circle in cartoon with major retinal blood vessels emerging from the superior and inferior edges). The small $\times$ in the cartoon indicates the fovea.

cholecystokinin precursor-positive S cone on-bipolar cells, and recoverin-positive cone off-bipolar cells in areas that retained cones. The inner plexiform layer was labeled with anti-γ-aminobutyric acid, but few γ-aminobutyric acid-positive amacrine cells were identified. Throughout the retina, the Müller and RPE cells were cellular retinaldehyde-binding protein positive, and the Müller cells were hypertrophied with increased glial fibrillary acidic protein immunolabeling, consistent with the observed loss of neurons (29). Sections treated with secondary antibodies alone had only autofluorescent lipofuscin granules in the RPE.

Morphometry. The total number of cones per 600 μm was increased in the *NR2E3* mutant retina (mean = 113.3) compared with the normal retina (mean = 54.1) (Fig. 3). The *NR2E3*

mutant retina contained fewer L/M cones (mean = 16.7, 14.7%) than the normal retina (mean = 45.3, 83.7%). The *NR2E3* mutant retina had increased numbers of S cones (mean = 103.7, 91.5%) compared with the normal retina (mean = 8.8, 16.3%). The sum of S and L/M cones (mean = 120.4) was higher than the total cone count (mean = 113.3) in the *NR2E3* mutant retina because some L/M cones coexpressed S cone opsin. In comparison, the retinitis pigmentosa retina contained very few cones (mean = 3). The differences in cone counts were significant for the total cones in normal (mean = 54.1) and ESCS (mean = 113.3) retinas ($P < 0.0001$) and for the S cones in the normal (mean = 8.8, 16.3%) and ESCS (mean = 103.7, 91.5%) retinas ($P < 0.0001$).

Discussion

Members of the superfamily of nuclear receptor transcription factors have roles in nervous system development of invertebrates and vertebrates (5, 30) and are important in the complex mechanisms that specify unique properties of developing neurons (31). The question posed in the present study was whether *NR2E3*, like the structurally closely related *NR2E1* (32–34), is also implicated in cell-fate determination, specifically in the human retina. Our phenotypic analyses with immunocytochemistry and morphometry in the retina from a patient homozygous for the R311Q *NR2E3* mutation (9) support the notion that this orphan nuclear receptor plays an important role in human retinal development and that this mutation leads to abnormal cone photoreceptor differentiation. This conclusion is concordant with recent evidence of defective retinal morphogenesis in *Nr2e3* and *Nr2e1* mutant mice (19, 20, 32).

The *NR2E3* mutant retina had several features not previously reported in humans: (*i*) an abnormal ratio of S to L/M cones, (*ii*) the presence of cones coexpressing S and L/M opsin in adult retina, and (*iii*) twice normal cone density in the central retina.

The abnormal ratio of S to L/M cones in this *NR2E3* mutant retina provides a morphological basis for the abnormal S to L/M cone relationship of psychophysical thresholds in the same patient, as well as other patients with the R311Q mutation. This may also be the basis of the photoreceptor ERG responses in other ESCS patients with different *NR2E3* mutations (11, 14–16). Nonhuman mammalian retinas examined with immunocytochemistry after undergoing physical or genetically engineered manipulation during development have also been reported to show abnormal ratios of cone subtypes. For example, embryonic and early postnatal rabbit and mouse retinal transplants develop a high ratio of S to M cones (reviewed in ref. 17). A thyroid hormone receptor is required for M cone development in mice, and animals lacking *Thrb* develop only S (UV) cones (35). Another recent study in mice indicates that lack of a nuclear transcription protein, Nrl, which is known to regulate rhodopsin expression (8), also results in increased numbers of S (UV) cones (36). Of high relevance to the present human results are the findings of increased numbers of S cones and retinal degeneration in the *rd7*/*rd7* mouse, known to have a deletion mutation involving part of the ligand-binding domain of the *Nr2e3* gene (19, 20).

In human fetal retinas, S cone opsin is expressed before L/M cone opsin (37). The *NR2E3* mutation resulted in decreased numbers of L/M cones, suggesting that some cone progenitor cells either failed to switch from the S to the L/M cone pathway or switched from the L/M to the S cone phenotype. In addition, about half of the L/M cones coexpressed S cone opsin in the *NR2E3* mutant retina. There is precedent for this. In rodents, M cones express S opsin before M opsin, and some cones synthesize both opsins throughout life (38–41). A more recent study (42) indicates that the majority of mouse cones express both S and M cone pigments. However, this seems not to be the case in humans, where some fetal cones coexpress S and L/M cone opsin, but very few adult cones express both opsins (37). The number of cones expressing S and L/M cone opsin was much higher than normal in the *NR2E3* mutant retina examined here. We looked for but did not find any cones coexpressing S and L/M opsin in the normal retina in the present study.

An increased number of cones in the retinal area examined is the third novel feature of the *NR2E3* mutant human retina. Rods were absent from this retina, and although the total number of cones was increased 2-fold, it is not possible at this point to determine whether the increased number of S cones includes rod progenitor cells that lacked the normal signal to become rods. Severely abnormal rod function is a feature of the ESCS phenotype at all ages tested (11), and it is possible that cells normally fated to become rods instead became S cones. Defective centrifugal migration of photoreceptors during development of the human central retina (43, 44) may also have contributed to this result.

Retinal degeneration is definitely a part of the R311Q *NR2E3* phenotype, based on histopathology and noninvasive studies. The histopathological hallmarks of retinal degeneration included ongoing cone cell loss, Müller cell gliosis, and RPE migration to the inner retina (27, 29). In our cross-sectional analysis of phenotype in ESCS patients with this *NR2E3* mutation, there was ophthalmoscopic, psychophysical, and ERG evidence of degeneration. In patients with retained peripheral retinal function, there was regional retinal variation of disease with more severe loss of S and L/M cone function in the near midperipheral retina than centrally or further in the periphery. Longitudinal study of S and L/M cone sensitivity in an *NR2E3* R311Q homozygote showed progressive losses over a decade.

A simple model of the phenotype of this *NR2E3* mutation would have two components: (*i*) a developmental effect leading to an abnormal ratio of S to L/M cones and the unique ESCS defect detected noninvasively; and (*ii*) variable retinal degeneration (45). The variable severity of degeneration in ESCS has caused confusion in the clinical literature, and several different diagnoses, from stationary night blindness to retinitis pigmentosa, have been applied to patients now known to have ESCS. An understated but key finding in our study that identified *NR2E3* as the cause of ESCS was that the patients in the sample shared the mechanism of abnormal S to L/M cone ratio but varied dramatically in degree of retinal degeneration (9). Although the temporal expression of *NR2E3* in human fetal retina is not known, murine data for *Nr2e3* suggest an embryonic (E18.5) phase and a postnatal (P2.5) phase extending into adulthood (20). The later phase may reflect the known fragility of S cones (46) or a role of *NR2E3* in maintenance of mature photoreceptors (20). As details become known about this aspect of *NR2E3* function, the retinal degeneration component of the disease expression may become amenable to therapeutic intervention.

We are grateful to the scientists who provided antibodies, Ms. J. Fisher for assistance with the tissue donations, Dr. N. Syed for advice on the gross pathology, Ms. L. M. Gardner for data analyses, Dr. X.-Y. Zhao for confocal microscopy help, and Dr. B. Reese for scientific input. This work was supported by Public Health Service Research Grants EY-05627 and EY-13203 (Bethesda), the Foundation Fighting Blindness (Owings Mills, MD), the F. M. Kirby Foundation, the Macula Vision Research Foundation (West Conshohocken, PA), the Macular Disease Foundation, the Fight for Sight research division of Prevent Blindness America (Schaumburg, IL), Research to Prevent Blindness (New York), and the Mackall Trust (New York). A.V.C. is a Research to Prevent Blindness William and Mary Greve Scholar. V.C.S. is an Associate Investigator of the Howard Hughes Medical Institute. S.G.J. is a Research to Prevent Blindness Senior Scientific Investigator.

1. Livesey, F. J. & Cepko, C. L. (2001) *Nat. Rev.* **2,** 109–118.
2. Rothermel, A. & Layer, P. G. (2001) *Eur. J. Neurosci.* **13,** 949–958.
3. Johnson, P. T., Williams, R. R. & Reese, B. E. (2001) *Visual Neurosci.* **18,** 157–168.
4. Egea, P. F., Klaholz, P. & Moras, D. (2000) *FEBS Lett.* **476,** 62–67.
5. Kumar, R. & Thompson, E. B. (1999) *Steroids* **64,** 310–319.
6. Kobayashi, M., Takezawa, S.-I., Hara, K., Yu, R. T., Umesono, Y., Agata, K., Taniwaki, M., Yasuda, K. & Ymesono, K. (1999) *Proc. Natl. Acad. Sci. USA* **96,** 4814–4819.
7. Mitton, K. P., Swain, P. K., Chen, S., Xu, S., Zack, D. J. & Swaroop, A. (2000) *J. Biol. Chem.* **275,** 29794–29799.
8. Swain, P. K., Hicks, D., Mears, A. J., Apell, I. J., Smith, J. E., John, S. K., Hendrickson, A., Milam, A. H. & Swaroop, A. (2001) *J. Biol. Chem.* **276,** 36824–36830.
9. Haider, N. B., Jacobson, S. G., Cideciyan, A. V., Swiderski, R., Streb, L. M., Searby, C., Beck, G., Hockey, R., Hanna, D. B., Gorman, S., *et al.* (2000) *Nat. Genet.* **24,** 127–131.
10. Miano, M. G., Jacobson, S. G., Carothers, A., Hanson, I., Teague, P., Lovell, J., Cideciyan, A. V., Haider, N., Stone, E. M., Sheffield, V. C. & Wright, A. F. (2000) *Am. J. Hum. Genet.* **67,** 1348–1351.
11. Jacobson, S. G., Marmor, M. F., Kemp, C. M. & Knighton, R. W. (1990) *Invest. Ophthalmol. Visual Sci.* **31,** 827–838.
12. Clarke, G., Heon, E. & McInnes, R. R. (2000) *Clin. Genet.* **57,** 313–329.
13. Curcio, C. A., Allen, K. A., Sloan, K. R., Lerea, C. L., Hurley, J. B., Klock, I. B. & Milam, A. H. (1991) *J. Comp. Neurol.* **312,** 610–624.
14. Jacobson, S. G., Roman, A. J., Roman, M. I., Gass, J. D. M. & Parker, J. A. (1991) *Am. J. Ophthalmol.* **111,** 446–453.
15. Roman, A. J. & Jacobson, S. G. (1991) *Exp. Eye Res.* **53,** 685–690.
16. Hood, D. C., Cideciyan, A. V., Roman, A. J. & Jacobson, S. G. (1995) *Vision Res.* **35,** 1473–1481.
17. Szel, A., Lukats, A., Fekete, T., Szepessy, Z. & Rohlich, P. (2000) *J. Opt. Soc. Am. A* **17,** 568–579.
18. Cepko, C. (2000) *Nat. Genet.* **24,** 99–100.
19. Akhmedov, N. B., Piriev, N. I., Chang, B., Rapoport, A. L., Hawes, N. L., Nishina, P. M., Nusinowitz, S., Heckenlively, J. R., Roderick, T. H., Kozak, C. A., *et al.* (2000) *Proc. Natl. Acad. Sci. USA* **97,** 5551–5556.
20. Haider, N. B., Naggert, J. K. & Nishina, P. M. (2001) *Hum. Mol. Genet.* **10,** 1619–1626.
21. Marmor, M., Jacobson, S. G., Foerster, M., Kellner, U. & Weleber, R. (1990) *Am. J. Ophthalmol.* **110,** 124–134.
22. Greenstein, V. C., Zaidi, Q., Hood, D. C., Spehar, B., Cideciyan, A. V. & Jacobson, S. G. (1996) *Vision Res.* **36,** 3711–3722.
23. Li, Z.-Y., Jacobson, S. G. & Milam, A. H. (1994) *Exp. Eye Res.* **58,** 397–408.
24. Milam, A. H. & Jacobson, S. G. (1990) *Ophthalmology* **97,** 1620–1631.
25. Milam, A. H. (2000) *Methods Mol. Med.* **47,** 71–88.
26. Li, Z.-Y., Kljavin, I. J. & Milam, A. H. (1995) *J. Neurosci.* **15,** 5429–5438.
27. Li, Z.-Y., Possin, D. E. & Milam, A. H. (1995) *Ophthalmology* **102,** 805–816.
28. John, S. K., Smith, J. E., Aguirre, G. D. & Milam, A. H. (2000) *Mol. Vision* **6,** 204–215.
29. Milam, A. H., Li, Z.-Y. & Fariss, R. N. (1998) *Prog. Ret. Eye Res.* **17,** 175–205.
30. Thummel, C. S. (1995) *Cell* **83,** 871–877.
31. Much, J. W., Slade, D. J., Klampert, K., Garriga, G. & Wightman, B. (2000) *Development (Cambridge, U.K.)* **127,** 703–712.
32. Yu, R. T., Chiang, M.-Y., Tanabe, T., Kobayashi, M., Yasuda, K., Evans, R. M. & Umesono, K. (2000) *Proc. Natl. Acad. Sci. USA* **97,** 2621–2625. (First Published March 7, 2000; 10.1073/pnas.050566897)
33. Yu, R. T., McKeown, M., Evans, R. M. & Umesono, K. (1994) *Nature (London)* **370,** 375–379.
34. Daniel, A., Dumstrei, K., Lenyel, J. A. & Hartenstein, V. (1999) *Development (Cambridge, U.K.)* **126,** 2945–2954.
35. Ng, L., Hurley, J. B., Dierks, B., Srivinas, M., Salto, C., Vennstrom, B., Reh, T. A. & Forrest, D. (2001) *Nat. Genet.* **27,** 94–98.
36. Mears, A. J., Kondo, M., Swain, P. K., Takada, Y., Bush, R. A., Saunders, T. L., Sieving, P. A. & Swaroop, A. (2001) *Nat. Genet.* **29,** 447–452.
37. Xiao, M. & Hendrickson, A. (2000) *J. Comp. Neurol.* **425,** 545–559.
38. Szel, A., van Veen, T. & Rohlich, P. (1994) *Nature (London)* **370,** 336.
39. Rohlich, P., van Veen, T. & Szel, A. (1994) *Neuron* **13,** 1159–1166.
40. Gloesman, M. & Ahnelt, P. K. (1998) *Invest. Ophthalmol. Visual Sci.* **39,** S1059.
41. Lyubarsky, A. L., Falsini, B., Pennesi, M. E., Valentini, P. & Pugh, E. N., Jr. (1999) *J. Neurosci.* **19,** 442–455.
42. Applebury, M. L., Antoch, M. P., Baxter, L. C., Chun, L. L., Falk, J. D., Farhangfar, F., Kage, K., Krzystolik, M. G., Lyass, L. A. & Robbins, J. T. (2000) *Neuron* **27,** 513–523.
43. Yuodelis, C. & Hendrickson, A. E. (1986) *Vision Res.* **26,** 847–856.
44. Provis, J. M., Diaz, C. M. & Dreher, B. (1998) *Prog. Neurobiol.* **54,** 549–580.
45. Marmor, M. F., Tan, F., Sutter, E. E. & Bearse, M. A., Jr. (1999) *Invest. Ophthalmol. Visual Sci.* **40,** 1866–1873.
46. de Monasterio, F. M., Schein, S. J. & McCrane, E. P. (1981) *Science* **213,** 1278–1281.